ISG15 is associated with cervical cancer development

PINGPING TAO[1*], LIYAN SUN[1*], YANMEI SUN[1], YUHUA WANG[1], YUMEI YANG[1], BINLIE YANG[1] and FANG LI[2]

[1]Department of Obstetrics and Gynecology, Pudong New Area People's Hospital Affiliated to Shanghai Health University, Shanghai 201299; [2]Department of Obstetrics and Gynecology, East Hospital, Tongji University School of Medicine, Shanghai 201999, P.R. China

Abstract. Cervical cancer (CC) is a complex disease. Numerous factors contribute to the tumourigenesis and progression of CC neoplasms. The present study analysed transcriptomic differences and simulated tumour progression to explore the pathogenesis of CC. RNA sequencing was performed to analyse the transcriptomic differences among normal tissue (NC), paracarcinoma tissue (TP), and primary tumour tissue (TT). Pseudo-time analysis was performed to simulate tumour progression. Reverse transcription-quantitative PCR (RT-qPCR) and immunohistochemistry (IHC) were used to analyse the expression levels of ISG15 ubiquitin-like modifier (*ISG15*). Cell proliferation wound healing and Transwell assays were used to examine the effect of *ISG15* inhibition and overexpression on HeLa cells. The RT-qPCR and IHC results indicated that *ISG15* expression was significantly upregulated in TT. An increasing trend of *ISG15* expression from NC to TP to TT was observed, which suggested that elevated *ISG15* expression was closely associated with malignant evolution in CC tissues. HeLa cell experiments revealed that *ISG15*-small interfering RNA inhibited cell proliferation and invasion. The present study demonstrated that *ISG15* was upregulated in CC and positively associated with the development of CC. *ISG15* may act as an oncogene in the tumourigenesis of CC.

Correspondence to: Dr Binlie Yang, Department of Obstetrics and Gynecology, Pudong New Area People's Hospital Affiliated to Shanghai Health University, 490 Chuanhuan South Road, Pudong New District, Shanghai 201299, P.R. China
E-mail: yangbl9@163.com

Professor Fang Li, Department of Obstetrics and Gynecology, East Hospital, Tongji University School of Medicine, 150 Jimo Road, Pudong New District, Shanghai 201999, P.R. China
E-mail: fang_li@tongji.edu.cn

*Contributed equally

Introduction

Cervical cancer (CC) is the fourth most common female malignancy worldwide (1,2). More than half a million women are diagnosed with CC, and the disease results in over 300,000 deaths worldwide each year (1,2). CC is a complex disease. In addition to infection with the well-studied human papillomavirus (HPV), numerous other factors can contribute to the tumourigenesis and progression of neoplasms (3,4). Aberrant genes, multiparity and smoking may impact the risk of CC (3,4). Several studies have demonstrated that the products of IFN-stimulated genes (ISGs) serve a pivotal role in HPV infection (5,6). The pathogenesis of CC is still unclear and probably involves the aberrant expression of numerous oncogenes and tumour suppressors (4). Therefore, an extended understanding of the gene expression program in CC will help us fight this devastating disease.

RNA sequencing (RNA-seq) has been used to rapidly generate a large amount of data on the gene expression landscape of CC (7-10). Differential expression (DE) analysis is the most common and straightforward analysis for a gene expression dataset. Using DE analysis, a set of highly upregulated and downregulated genes can be identified by comparing primary tumour tissue (TT) and paracarcinoma tissue (TP). Although these studies have provided significant findings for CC, most studies have lacked normal tissue (NC) samples as a reference to allow the analysis of tumour progression of CC from NC to TP to TT (7-10).

In the present study, RNA-seq was performed to analyse genes that are dysregulated in CC. The relationship between aberrant RNA expression profiles and disease states was also analysed. Furthermore, Gene Ontology (GO) and Kyoto Encyclopedia of Genes and Genomes (KEGG) analyses were conducted to annotate the differentially expressed genes (DEGs). The present study further analysed the tumour evolution trajectory using pseudo-time analysis. Finally, a cell assay was performed to examine the effect of ISG15 ubiquitin-like modifier (ISG15 inhibition and overexpression) on HeLa cells. The results of the present study could guide targeted drug research for CC therapies.

Materials and methods

Samples. Samples (Table I) from female patients (age range, 27-70 years; mean age, 50.36±13.26 years) with cervical

cancer surgery were stored in a -80°C freezer. The inclusion criteria were as follows: i) The pathological diagnosis was clearly cervical squamous cell carcinoma; ii) clinical data were complete, including age, tumour clinical stage, grade, pathological type, infiltration and lymph node metastasis (11); iii) no history of physical therapy or preoperative chemoradiotherapy; and iv) clinical FIGO (2018) stage IB1 to IIA2 (12). Exclusion criteria were as follows: i) Case data were incomplete; ii) combined immune diseases and other malignant tumours; iii) a history of adjuvant chemotherapy and radiotherapy before surgery; iv) the use of pathological case data without the informed consent of the patient; v) pathological diagnosis was of another type of cervical cancer; and vi) the surgical method did not meet the requirements. The experiment was performed by comparative sequencing analysis using RNA-seq data from TT, TP (2 cm ≤ TP ≥0.5 cm from the tumour tissue) and NC (≥2 cm away from the tumour tissue) samples collected from 14 patients with CC who underwent surgery at Pudong New Area People's Hospital Affiliated to Shanghai Health University (Shanghai, China) between January 2019 and June 2020. All patients had CC at stages IB1-IIA2 (based on the Criteria for Clinical Staging of Cervical Carcinoma 2018 Modified Version of the International Federation of Gynecology and Obstetrics) and underwent wide hysterectomy and lymphadenectomy in the pelvic cavity. These patients were divided into the high ISG15 expression group and the low ISG15 expression group according to the median ISG15 gene expression level in TT tissue. The clinical data of these patients, such as age, BMI and tumor markers, were then collected.

The study was approved by the Ethical Committee of the People's Hospital of Shanghai Pudong New District (PRYLL-QKJW1703&PKJ2021-Y21; Shanghai, China). Written informed consent was provided by each of the patients or their guardians (if the patient was under the legal age to provide consent or otherwise incapacitated or deceased), and all procedures were conducted according to the Helsinki Ethical Principles for medical research.

RNA-seq and data analysis. A TRIzol® kit (Invitrogen; Thermo Fisher Scientific, Inc.) was used to purify the RNA from the samples. For RNA extraction, tissues were lysed with 1 ml TRIzol reagent per 50-100 mg sample. For RNA extraction, the cells were first precipitated by centrifugation at 500 x g (4°C) for 5 min and then 1 ml TRIzol was added every 5-10x10⁶ cells, and the mixture was agitated 2-3 times to ensure complete cell lysis. The TRIzol lysate was transferred into EP tubes and placed at room temperature for 5 min. A total of 0.2 ml chloroform was added for every 1 ml TRIzol, followed by agitation for 15 sec, being placed at room temperature for 2-3 min, and then centrifugation at 12,000 x g (2-8°C) for 15 min. The upper aqueous phase was removed and placed in a new EP tube with an equal volume of isopropanol, and then placed at room temperature for 10 min, before centrifugation at 12,000 x g (2-8°C) for 10 min. The supernatant was discarded and washed with 1 ml 75% ethanol per 1 ml TRIzol, mixed by vortex, centrifuged at 7,500 g (2-8°C) for 5 min, and then the supernatant was discarded. The precipitated RNA was allowed to dissolve the RNA precipitate with RNase-free water at room temperature after natural drying. Reverse transcription of RNA samples was used to prepare cDNA using the SmartScribe™ Reverse Transcriptase kit (Takara Bio Inc.). VANTS DNA Clean Beads (Vazyme Biotech, Co., Ltd.) was used to sort cDNA products, and TruePrep DNA Library Prep Kit V2 for Illumina (Vazyme Biotech, Co., Ltd.) was used to obtain 200- to 1,000-bp fragments for preparing the cDNA library. All libraries were quantified using a 2100 Bioanalyzer and pooled at 1:1 at 2 nM for HiSeq 150 bp paired-end sequencing (Illumina, Inc.).

Data pre-processing, principal component analysis (PCA), and hierarchical clustering analysis were performed in R-4.12 (r-project.org) using the 'base' function and 'stat' package (version 4.1.2). DEGs were defined based on fold change (FC) and statistical significance using t-tests (FC >1.5 or <0.67; $P<0.05$). KEGG (https://www.genome.jp/kegg) pathway and GO (http://geneontology.org/) analyses were performed to identify biological functions associated with DEGs in Metascape (http://metascape.org/). The Cancer Genome Atlas (TCGA; https:// www.cancer.gov/about-nci/organization/ccg/research/structural-genomics/tcga) survival analysis was performed using OncoLnc (oncolnc.org). Co-expression networks were built by computing the correlation coefficient of DEGs (cor >0.8) and mapped using Cytoscape software (version 3.6.1; https://cytoscape.org/). Pseudo-time trajectory analysis was implemented using the Monocle package (version 2.22.0; https://bioconductor.org/packages/release/bioc/html/monocle.html) in R to investigate the evolution of CC. To explore the interactions of the top evolutionary trajectory genes, the genes were submitted to Search Tool for the Retrieval of Interacting Genes/Proteins (version 11.5; http://string.embl.de/) to build protein-protein interaction (PPI) networks.

Reverse transcription-quantitative PCR (RT-qPCR). A TRIzol kit (Invitrogen; Thermo Fisher Scientific, Inc.) was used to purify the RNA from the tissue or cells. ReverTra Ace® qPCR RT Kit (Toyobo Life Science) was used at 42°C for 18 min and 98°C 5 min for the reverse transcription of RNA to cDNA. The primers were designed and synthesized by General Biotech Co., Ltd. RT-qPCR was performed using the KAPA SYBR Green SuperMix PCR kit (Kapa Biosystems; Roche Diagnostics) and the AriaMx Real-Time PCR System (Agilent Technologies, Inc.). Reaction conditions were as follows: 95°C for 3 min, 95°C for 10 sec and 60°C for 30 sec, for 40 cycles. Differences in gene expression were calculated using the relative standard curve and comparative threshold cycle method ($2^{-\Delta\Delta Cq}$) (13), and RT-qPCR was used to verify the expression of GAPDH. The following primers were used: *GAPDH* forward, 5'-GCAAGTTCAACGGCACAGTCA-3' and reverse, 5'-ACGACATACTCAGCACCAGCAT-3'; and *ISG15* forward, 5'-ACAGCCATGGGCTGGGA-3' and reverse, 5'-GTTCGTCGCATTTGTCCACC-3'.

Immunohistochemistry (IHC). Samples were fixed in 10% Neutral Formalin Fix Solution (BBI Solutions), embedded in paraffin, and cut into 4-μm thick tissue sections. For antigen retrieval, tissue sections were placed in antigen retrieval buffer (pH 9.0; Wuhan Servicebio Technology, Co., Ltd.) for antigen retrieval in a microwave oven on medium power for 8 min until boiling, then cooled for 8 min and then switched to medium-low power for 7 min. After natural cooling, the slides were placed in PBS (pH 7.4; Wuhan Servicebio

Table I. Association between *ISG15* expression and clinicopathological features in cervical cancer.

Characteristics	High ISG15 expression (n=7)	Low ISG15 expression (n=7)	P-value (Fisher's exact test)	P-value (unpaired t-test)
Age, years	53.86±14.05	46.85±12.39		0.34
BMI	26.27±2.16	23.65±3.65		0.25
Staging, n (%)			0.0047	
I	0 (0.0)	6 (85.7)		
II	7 (100.0)	1 (14.3)		
Tumour size, n (%)			>0.99	
≥4 cm	2 (28.6)	3 (42.9)		
<4 cm	5 (71.4)	4 (57.1)		
Depth of infiltration, n (%)			>0.99	
≥1/2	5 (71.4)	4 (57.1)		
<1/2	2 (28.6)	3 (42.9)		
Tumour markers				
SCC antigen, ng/ml	10.43±18.44	1.42±1.33		0.26
CA125, U/ml	5.69±7.29	7.20±3.77		0.66
CA199, U/ml	18.66±18.22	13.85±7.96		0.56
AFP, ng/ml	11.58±11.59	5.30±5.23		0.25
CEA, ng/ml	7.04±5.03	2.79±3.25		0.10

ISG15, ISG15 ubiquitin-like modifier; SCC, squamous cell carcinoma.

Technology, Co., Ltd.) and washed 3 times on a destaining shaker. Next, 3% hydrogen peroxide solution was incubated with the sample at room temperature for 25 min to block endogenous peroxidase, followed by blocking with 3% BSA (Sangon Biotech, Co., Ltd.) at room temperature for 30 min. The tissue sections were incubated with anti-ISG15 antibody (dilution, 1:100; cat. no. DF6316; Affinity Biosciences) at room temperature (RT) for 1 h. The HRP-labelled goat-anti-rabbit (dilution, 1:200; cat. no. G1213; Wuhan Servicebio Technology, Co., Ltd.) antibody was used for incubation at RT for 1 h. After the 3,3'-diaminobenzidine application for 5-10 min, the staining was observed under a fluorescence microscope (CKX53; Olympus Corporation). The intensity was scored by eye as follows: 0, negative; 1, weak; 2, moderate; and 3, strong.

Transfection. Synthesized *ISG15* overexpression vector (500 ng/μl), small interfering RNA (siRNA; 20 pmol/μl), and scrambled siRNA controls (20 pmol/μl) were designed and synthesized by Shanghai GenePharma Co., Ltd. A total of 1x10^6 cells/well were seeded into 6-well plates and transfected with ISG15 overexpression and siRNA using HilyMax Reagent (Dojindo Laboratories, Inc.) according to the manufacturer's instructions. Transfection was performed using 120 μl Opti-MEM (Gibco; Thermo Fisher Scientific, Inc.), 80 pmol (4 μl) overexpression or siRNA, and 12 μl HilyMAX reagent at RT for 15 min. The plasmid or siRNA-Hilymax complex was added to the cells, then incubated at 37˚C for 6 h to complete transfection. The construction of transfected cell models was validated using RT-qPCR as aforementioned at 48 h after transfection.

The following ISG15 siRNA sequences and ISG15 overexpression were used: *ISG15* siRNA sense (5'-3'), GCACCAGCAUGAAGACAUATT and antisense (5'-3'), UAUGUCUUCAUGCUGGUGCTT; scrambled siRNA control sense (5'-3'), UUCUCCGAACGUGUCACGUTT and antisense (5'-3'), ACGUGACACGUUCGGAGAATT; *ISG15* overexpression: ATGGGCTGGGACCTGACGGTGAAGATGCTGGCGGGCAACGAATTCCAGGTGTCCCTGAGCAGCTCCATGTCGGTGTCAGAGCTGAAGGCGCAGATCACCCAGAAGATCGGCGTGCACGCCTTCCAGCAGCGTCTGGCTGTCCACCCGAGCGGTGTGGCGCTGCAGGACAGGGTCCCCCTTGCCAGCCAGGGCCTGGGCCCCGGCAGCACGGTCCTGCTGGTGGTGGACAAATGCGACGAACCTCTGAGCATCCTGGTGAGGAATAACAAGGGCCGCAGCAGCACCTACGAGGTACGGCTGACGCAGACCGTGGCCCACCTGAAGCAGCAAGTGAGCGGGCTGGAGGGTGTGCAGGACGACCTGTTCTGGCTGACCTTCGAGGGGAAGCCCCTGGAGGACCAGCTCCCGCTGGGGGAGTACGGCCTCAAGCCCCTGAGCACCGTGTTCATGAATCTGCGCCTGCGGGGAGGCGGCACAGAGCCTGGCGGGCGGAGCTAA.

Western blotting. Total protein was extracted from CC tissues using RIPA buffer containing protease and phosphatase inhibitor cocktail (both from Sigma-Aldrich; Merck KGaA). The protein concentration was determined using a BCA Protein Assay kit (Beyotime Institute of Biotechnology). Proteins (50 μg/lane) were separated on 10% SDS-PAGE and transferred to PVDF membranes. The membranes were blocked with 5% skimmed milk and 0.1% Tween-20 in Tris-buffered saline for 2 h at RT. Membranes were probed at 4˚C overnight with primary antibodies against ISG15 (dilution, 1:5,000; cat. no. ab133346;

Abcam) and GAPDH (dilution, 1:2,500; cat. no. ab9485; Abcam). After washing in PBST (0.5% Tween-20) three times, the blots were incubated with HRP-conjugated anti-rabbit secondary antibodies (dilution, 1:5,000; cat. no. ab205718; Abcam) for 1 h at RT. The signal was visualized using ECL western blotting detection reagents (Tanon Science and Technology Co., Ltd.). Protein expression levels were quantified using ImageJ software (version 1.50; National Institutes of Health).

CCK8 proliferation assay. The transfected cells were placed at a density of $1x10^4$ cells per well on a 96-well cell culture plate, which was placed in a 37˚C cell culture incubator and incubated overnight. The old culture medium was removed from the 96-well plate, and 100 μl DMEM (Gibco; Thermo Fisher Scientific, Inc.) was added to each well. The change in proliferation capacity of each group of cells was detected by the CCK-8 method at 0, 24, 48 and 72 h after the liquid change. The old solution was discarded and 95 μl medium and 5 μl Cell Counting Kit-8 (CCK-8) reagent (Dojindo Laboratories, Inc.) was added to each well of the 96-well plate to be tested and incubated at 37˚C for 1-3 h. The OD of each well was measured at 450 nm using a microplate reader.

Wound-healing assay. The transfected cells (serum starved) were placed at a density of $2x10^5$ cells per well on a 24-well cell culture plate, which was placed in a 37˚C cell culture incubator and incubated overnight. When they had reached 80% confluence, a 10-μl pipette tip was used to scratch a line on the cell layer. The cells that had migrated into the wound area were imaged under a fluorescence microscope (CKX53; Olympus Corporation) at 0 and 24 h. The distance migrated by the cell monolayer to close the wounded area during this time period was measured, Results were expressed as a migration index, i.e., the distance migrated by the ISG15-siRNA or ISG15-OE group relative to the distance migrated by control group.

Transwell assay. A Transwell chamber (24 well; 8.0 μm pores) was used for the invasion assay. The matrigel was diluted in serum-free medium (Matrigel:serum-free medium, 1:8) at 4˚C, and then the diluted Matrigel was added into the wells (upper chamber) for incubation at 37˚C for 4 h. HeLa ($5x10^4$) cells were seeded into the prepared upper chamber containing DMEM without serum at 37˚C for 30 min, and 500 μl complete medium (DMEM and 10% FBS) was added to the lower chamber, following routine procedures. After 48 h, cells invading the lower chamber were collected, fixed with 5% glutaraldehyde for 10 min at room temperature, stained with 0.5% crystal violet for 15 min at room temperature, and then counted under a microscope (CKX53; Olympus Corporation).

Statistical analysis. Statistical analysis was performed using GraphPad Prism software (version 7.0; GraphPad Software, Inc.), and quantitative data are presented as the mean ± standard deviation of three independent experiments. The difference in the levels of ISG15 expression was calculated using Fisher's exact test. One-way ANOVA followed by Tukey's post hoc test was used for comparisons among groups. Differences between high ISG15 expression and low ISG15 expression groups were analyzed using an unpaired t-test. P<0.05 was considered to indicate a statistically significant difference.

Results

Transcriptome sequencing data analysis. The PCA diagram shows an obvious distinction between TT, TP and NC tissue (Fig. 1A and B). To investigate transcriptomic differences between TT and TP, the DEGs between the two groups were analysed. DEG analysis revealed that there were 1,405 upregulated DEGs and 1,256 downregulated DEGs in the TT group compared with the TP group (Fig. 1C and D). Furthermore, KEGG pathway and GO analyses of the DEGs were performed. KEGG analysis demonstrated that the pathways such as 'focal adhesion', 'ECM-receptor interaction', 'vascular smooth muscle contraction', 'PI3K-Akt signalling pathway' and 'pathways in cancer' were enriched, among others. Additionally, GO analysis revealed the functional enrichment of pathways such as 'cell adhesion', among others (Fig. 1E). The co-network analysis indicated that transcription factors, such as myocyte enhancer factor 2C, interferon regulatory factor 6 and high mobility group AT-hook 1, have regulatory effects on DEGs (Fig. 1F).

RNA-seq data reflect disease states and stages. A graph was plotted based on a discriminative dimensionality reduction tree analysis using the Monocle package to demonstrate the developmental path of CC. The trajectory had a tree structure with NC as the root state. The graph depicts the tree best fitted to the CC developmental trajectory. The solid black line represents the main route of the minimal spanning tree constructed, which exhibited the backbone and order of CC development along a pseudo-temporal continuum (NC-TP-TT; Fig. 2A). The top turning point-enriched genes, such as *ISG15*, acyl-CoA thioesterase 7 and ribosomal protein L22, are shown in Fig. 2B. A PPI network was constructed from these genes, and it was revealed that *ISG15* had a significant regulatory role (Fig. 2C). Functional analysis revealed significant enrichment of the 'cell adhesion molecules (CAMs)' pathway and 'cell adhesion' (Fig. 2D).

Validation of the significance of ISG15 expression in CC. TCGA survival (14) analysis demonstrated that *ISG15* expression had no significant effect on the prognosis of patients with CC (Fig. 3A). RT-qPCR (Fig. 3B) and IHC assays (Fig. 3C) were performed to verify the regulatory relationships among NC, TP and TT. The results revealed that *ISG15* expression was significantly higher in the TT group compared with that in the TP group. In addition, RT-qPCR assays demonstrated that the *ISG15* expression in the TP group was higher than that in the NC group. As shown in Table I, the associations between *ISG15* and the clinical features of CC indicated that *ISG15* expression was significantly associated with tumour stage (P=0.0047).

ISG15-siRNA inhibits the proliferation and invasion of HeLa cells. To further investigate the effect of *ISG15* on CC cell proliferation and migration, *ISG15* interference experiments were performed using HeLa cells *in vitro*. The results of transfection showed that ISG15 expression was reduced in cells transfected with ISG15 siRNA compared with the siRNA negative control (P<0.01). Similarly, ISG15 expression was increased in cells transfected with the ISG15 overexpression vector (ISG15-OE)
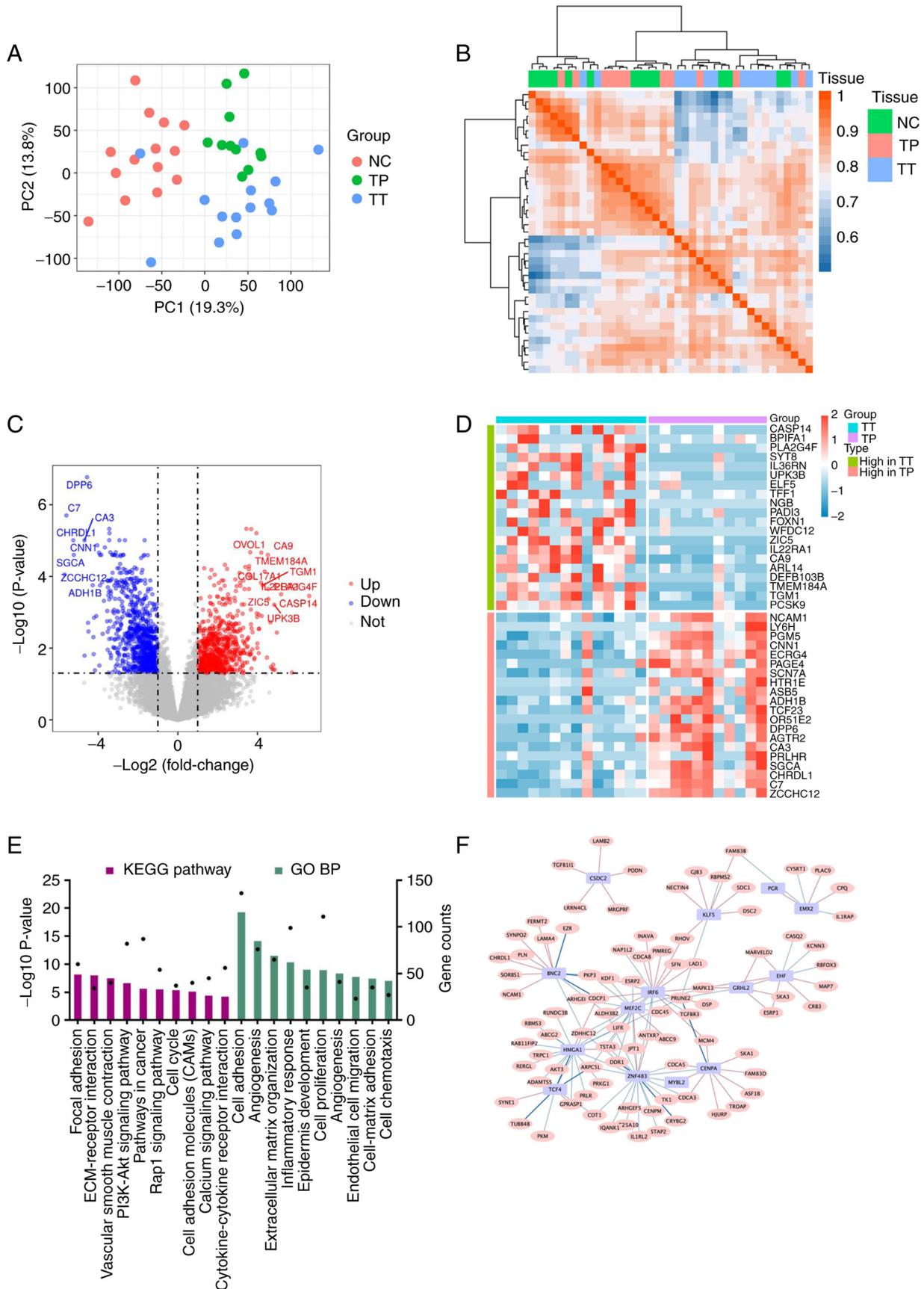
Figure 1. RNA sequencing analysis reveals the heterogeneity of NC, TP and TT. (A) PC analysis and (B) hierarchical clustering analysis revealed an obvious distinction between tumour and non-tumour tissues. (C) Volcano plot showing the DEGs between TT and TP. (D) Top 20 DEGs in TT vs. TP; (E) KEGG pathway and GO BP analysis of DEGs in TT vs. TP showing P-values (black dots) and gene counts (bars). (F) Gene co-expression network analysis showing the key transcription factors and DEGs between TT and TP (purple rectangles represent the key transcription factors; pink ovals represent DEGs; pink lines represent positive correlations; and blue lines represent negative correlations); BP, biological process; DEGs, differentially expressed genes; GO, Gene Ontology; KEGG, Kyoto Encyclopedia of Genes and Genomes; NC, normal tissue; PC, principal component; TP, paracarcinoma tissue; TT, primary tumour tissue.
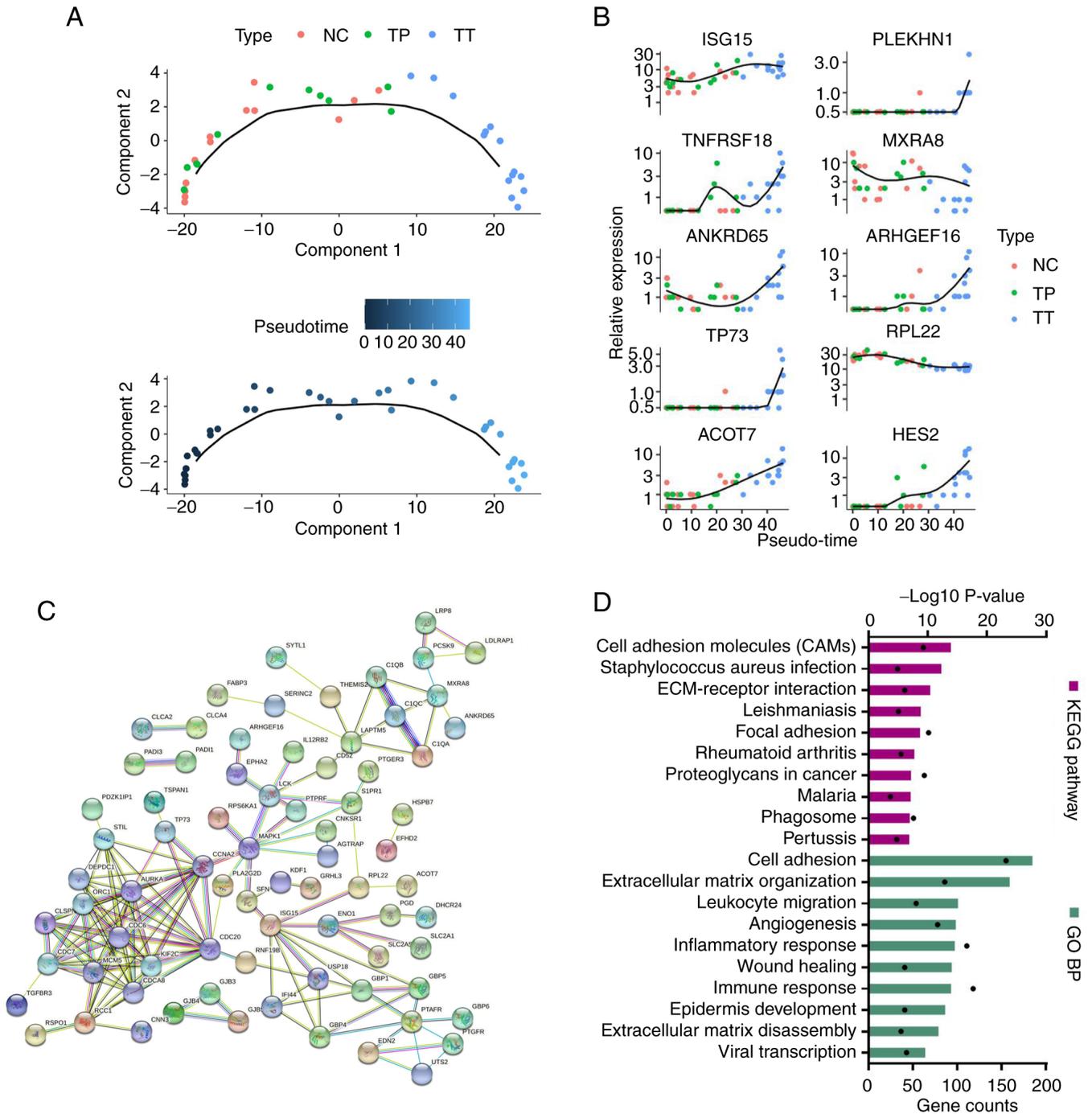
Figure 2. RNA sequencing data reflected disease states and stages. (A) Pseudo-time trajectory analysis of cervical cancer development. (B) Top turning point-enriched genes, such as *ISG15*, *ACOT7* and *RPL22*, in pseudo-time trajectory analysis. (C) Protein-protein interaction network showing that *ISG15* had a significant regulatory role. (D) KEGG pathway and GO BP analysis of turning point-enriched genes showing P-values (black dots) and gene counts (bars). *ACOT7*, acyl-CoA thioesterase 7; *ANKRD65*, ankyrin repeat domain 65; *ARHGEF16*, rho guanine nucleotide exchange factor 16; BP, biological process; GO, Gene Ontology; *HES2*, hes family bHLH transcription factor 2; *ISG15*, ISG15 ubiquitin-like modifier; KEGG, Kyoto Encyclopedia of Genes and Genomes; *MXRA8*, matrix remodeling associated 8; NC, normal tissue; *PLEKHN1*, pleckstrin homology domain containing N1; *RPL22*, ribosomal protein L22; *TNFRSF18*, TNF receptor superfamily member 18; TP, paracarcinoma tissue; *TP73*, tumour protein p73; TT, primary tumour tissue.

compared with the empty vector (P<0.001) (Fig. 3D). CCK-8 assays indicated that the inhibition of ISG15 significantly reduced the proliferation of HeLa cells (48 h; P<0.01), and overexpression of ISG15 significantly increased the proliferation of HeLa cells (48 h; P<0.05) compared with the control (Fig. 3E). Western blot analysis revealed a significant decrease in ISG15 expression in the ISG15-siRNA group compared with the control group (P<0.01) and upregulation of ISG15 in the ISG15-OE group (P<0.001)

(Fig. 3F). Scratch assays demonstrated that the inhibition of ISG15 effectively inhibited the migration of HeLa cells (P<0.05), and overexpression of ISG15 effectively promoted the migration of HeLa cells (P<0.05) compared with the control (Fig. 3G). In addition, Transwell assays revealed that invasion was significantly inhibited in the cells treated with ISG15-siRNA (P<0.001), and invasion was significantly promoted in the cells treated with ISG15-OE (P<0.001) compared with the control (Fig. 3H).
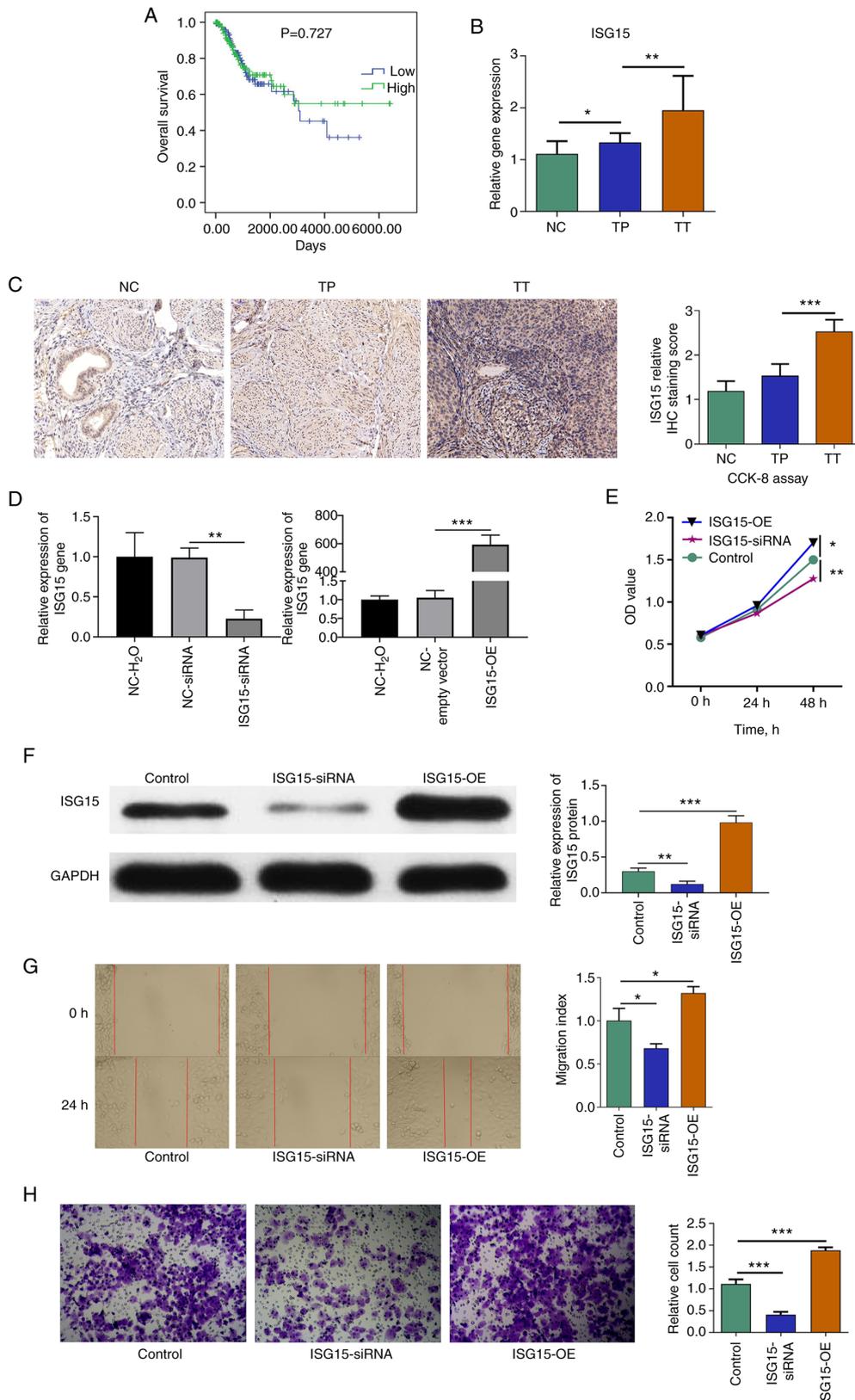
Figure 3. *ISG15* promotes the proliferation and invasion of HeLa cells. (A) The Cancer Genome Atlas survival analysis of ISG15. (B) Relative ISG15 expression in cervical cancer tissues. (C) IHC staining (x200 magnification) and ISG15 score. (D) RT-qPCR results demonstrated the success of the ISG15 interference assay, where ISG15 expression was reduced in cells transfected with ISG15 siRNA compared with the siRNA negative control (P<0.01); similarly, ISG15 expression was increased in cells transfected with the ISG15 overexpression vector compared with the empty vector (P<0.001). (E) A cell proliferation assay indicated that *ISG15* promoted the proliferation of HeLa cells. (F) Western blot analysis revealed a significant decrease in ISG15 expression in the ISG15 siRNA group compared with the control group (P<0.01) and an upregulation of ISG15 expression in the ISG15-OE group (P<0.001). (G) Cell scratch assays (x100 magnfication) demonstrated that inhibition of *ISG15* effectively inhibited the migration of HeLa cells. (H) Transwell assays (x100 magnification) revealed that invasion was significantly inhibited in the cells treated with *ISG15*-siRNA. *P<0.05, **P<0.01, ***P<0.001. CCK-8, Cell Counting Kit-8; IHC, immunohistochemistry; *ISG15*, ISG15 ubiquitin-like modifier; NC, normal tissue; OD, optical density; siRNA, small interfering RNA; TP, paracarcinoma tissue; TT, primary tumour tissue.

Discussion

In the present study, the transcriptomic differences among NC, TP, and TT tissues from patients with CC were analysed and tumour progression was simulated using pseudo-time analysis. It was observed that *ISG15* served a key role in the development of CC. The results of immunohistochemical and RT-qPCR assays indicated that *ISG15* expression was increased in TT. An increasing trend of *ISG15* expression from NC to TP to TT was also observed, which suggests that higher expression of *ISG15* was closely associated with the malignant evolution of CC tissues. HeLa cell experiments demonstrated that *ISG15*-siRNA inhibited cell proliferation and invasion.

ISG15 is one of the genes that are most highly induced in response to viral infection (15). A study has demonstrated that ISGylation of the HPV L1 capsid protein has a dominant inhibitory effect on the infectivity of HPV16 pseudoviruses (15). Cannella *et al* (16) observed higher *ISG15* expression in patients with CC with low-risk HPV infection than in those with high-risk HPV. Pierangeli *et al* (17) found that ISG15 expression was higher in low-risk HPV infection samples than in HPV-negative samples, while high-risk HPV infections had a low ISG15 level. Rajkumar *et al* (18) found that ISG15 was upregulated in patients with CC compared with normal controls, which was confirmed in the present study, suggesting that ISG15 may serve an important role in the progression of CC.

Several studies have provided evidence that *ISG15* and its conjugation are involved in cancer pathogenesis (19-22). *ISG15* is secreted or released by various cell types, including fibroblasts, neutrophils, monocytes, and lymphocytes. *ISG15* has emerged as a pivotal regulator in diverse cellular processes, including proliferation, apoptosis, and DNA repair. The receptor for extracellular *ISG15* has been identified as leukocyte function-associated antigen-1 (LFA-1), an adhesion molecule of the integrin family composed of an αL and $\beta 2$ subunit (23,24). LFA-1 binding to intercellular adhesion molecule 1 is critical in homing leukocytes to sites of inflammation (23,24). Elevated *ISG15* expression has been demonstrated to be required for tumourigenic phenotypes in triple-negative breast cancer (TNBC) possessing inactivated p53 and ADP ribosylation factor, suggesting the potential role of *ISG15* in TNBC development and progression (25). High levels of *ISG15* accelerate the invasion of breast cancer cells and are associated with poor prognosis in patients with breast cancer (25-28). *ISG15* and enzymes involved in ISGylation promote the proliferation and migration of hepatocellular carcinoma (HCC) by stabilizing apoptosis inhibitors (21,29). Furthermore, the expression of *ISG15* is higher in HBV-related HCC tissues than in non-tumour tissues (21,29). The expression of *ISG15* has been demonstrated to be elevated in oesophageal squamous cell carcinoma (ESCC) and to be closely associated with clinical outcomes, indicating that *ISG15* may be used as a prognostic biomarker in patients with ESCC (30).

The present results indicated that ISG15 promotes CC cell proliferation and invasion. *ISG15* may act as an oncogene in the tumourigenesis of CC. Taken together, these data demonstrate that *ISG15* serves pivotal roles in cancer cell proliferation and apoptotic cell death.

The limitation of the present study was the small number of patient cases enrolled. Survival analysis could not be performed because of the small sample size. However, ISG15 expression had no significant effect on the prognosis of patients with CC in TCGA data. In conclusion, the present study demonstrated that *ISG15* was upregulated in CC tumour tissue and positively associated with the development of CC. *ISG15* may be a potential anticancer drug target for future CC-targeted drug discovery.

Availability of data and materials

The datasets generated and/or analysed during the current study are available in the GEO database repository (GSE192804, https://www.ncbi.nlm.nih.gov/geo/query/acc.cgi?acc=GSE192804). All other data used and/or analyzed during the current study are available from the corresponding author on reasonable request.

Authors' contributions

PT, LS, FL and BY designed the research, performed the analyses and wrote the paper. YS, YW and YY performed experiments. PT and BY confirm the authenticity of all the raw data. All authors read and approved the final manuscript.

Ethics approval and consent to participate

All experiments were approved by the Ethics Committee of the Pudong New Area People's Hospital Affiliated to Shanghai Health University (PRYLL-QKJW1703; Shanghai, China). Written informed consent to participate in the study was obtained from each patient before they entered the study.

Patient consent for publication

Patient consent for publication was covered by the informed consent document.

Competing interests

The authors declare that they have no competing interests.

References

1. Cohen PA, Jhingran A, Oaknin A and Denny L: Cervical cancer. Lancet 393: 169-182, 2019.
2. Li H, Wu X and Cheng X: Advances in diagnosis and treatment of metastatic cervical cancer. J Gynecol Oncol 27: e43. 2016.
3. Wang H, Zhao Y, Chen M and Cui J: Identification of novel long non-coding and circular RNAs in human papillomavirus-mediated cervical cancer. Front Microbiol 8: 1720, 2017.
4. Choi YJ and Park JS: Clinical significance of human papillomavirus genotyping. J Gynecol Oncol 27: e21, 2016.

5. Stanley MA: Epithelial cell responses to infection with human papillomavirus. Clin Microbiol Rev 25: 215-222, 2012.
6. Hong S, Mehta KP and Laimins LA: Suppression of STAT-1 expression by human papillomaviruses is necessary for differentiation-dependent genome amplification and plasmid maintenance. J Virol 85: 9486-9494, 2011.
7. Li X, Tian R, Gao H, Yang Y, Williams BRG, Gantier MP, McMillan NAJ, Xu D, Hu Y and Gao Y: Identification of a histone family gene signature for predicting the prognosis of cervical cancer patients. Sci Rep 7: 16495, 2017.
8. Brant AC, Menezes AN, Felix SP, de Almeida LM, Sammeth M and Moreira MAM: Characterization of HPV integration, viral gene expression and E6E7 alternative transcripts by RNA-Seq: A descriptive study in invasive cervical cancer. Genomics 111: 1853-1861, 2019.
9. Gong Z, Liu J, Xie X, Xu X, Wu P, Li H, Wang Y, Li W and Xiong J: Identification of potential target genes of USP22 via ChIP-seq and RNA-seq analysis in HeLa cells. Genet Mol Biol 41: 488-495, 2018.
10. Yu B, Chen L, Zhang W, Li Y, Zhang Y, Gao Y, Teng X, Zou L, Wang Q, Jia H, et al: TOP2A and CENPF are synergistic master regulators activated in cervical cancer. BMC Med Genomics 13: 145, 2020.
11. Xu YP, Wang ZQ, Liang XD, Wang Y and Wang JL: Comparative analysis of the prognosis of patients with locally advanced cervical cancer undergoing laparoscopic or abdominal surgery. Zhonghua Fu Chan Ke Za Zhi 55: 609-616, 2020 (In Chinese).
12. Berek JS, Matsuo K, Grubbs BH, Gaffney DK, Lee SI, Kilcoyne A, Cheon GJ, Yoo CW, Li L, Shao Y, et al: Multidisciplinary perspectives on newly revised 2018 FIGO staging of cancer of the cervix uteri. J Gynecol Oncol 30: e40, 2019.
13. Livak KJ and Schmittgen TD: Analysis of relative gene expression data using real-time quantitative PCR and the 2(-Delta Delta C(T)) method. Methods 25: 402-408, 2001.
14. Anaya J: OncoLnc: Linking TCGA survival data to mRNAs, miRNAs, and lncRNAs. PeerJ Comput Sci 2: e67, 2016.
15. Durfee LA, Lyon N, Seo K and Huibregtse JM: The ISG15 conjugation system broadly targets newly synthesized proteins: Implications for the antiviral function of ISG15. Mol Cell 38: 722-732, 2010.
16. Cannella F, Scagnolari C, Selvaggi C, Stentella P, Recine N, Antonelli G and Pierangeli A: Interferon lambda 1 expression in cervical cells differs between low-risk and high-risk human papillomavirus-positive women. Med Microbiol Immunol 203: 177-184, 2014.
17. Pierangeli A, Degener AM, Ferreri ML, Riva E, Rizzo B, Turriziani O, Luciani S, Scagnolari C and Antonelli G: Interferon-induced gene expression in cervical mucosa during human papillomavirus infection. Int J Immunopathol Pharmacol 24: 217-223, 2011.
18. Rajkumar T, Sabitha K, Vijayalakshmi N, Shirley S, Bose MV, Gopal G and Selvaluxmy G: Identification and validation of genes involved in cervical tumourigenesis. BMC Cancer 11: 80, 2011.
19. Desai SD, Reed RE, Burks J, Wood LM, Pullikuth AK, Haas AL, Liu LF, Breslin JW, Meiners S and Sankar S: ISG15 disrupts cytoskeletal architecture and promotes motility in human breast cancer cells. Exp Biol Med (Maywood) 237: 38-49, 2012.
20. Kiessling A, Hogrefe C, Erb S, Bobach C, Fuessel S, Wessjohann L and Seliger B: Expression, regulation and function of the ISGylation system in prostate cancer. Oncogene 28: 2606-2620, 2009.
21. Li C, Wang J, Zhang H, Zhu M, Chen F, Hu Y, Liu H and Zhu H: Interferon-stimulated gene 15 (ISG15) is a trigger for tumorigenesis and metastasis of hepatocellular carcinoma. Oncotarget 5: 8429-8441, 2014.
22. Wood LM, Pan ZK, Seavey MM, Muthukumaran G and Paterson Y: The ubiquitin-like protein, ISG15, is a novel tumor-associated antigen for cancer immunotherapy. Cancer Immunol Immunother 61: 689-700, 2012.
23. Swaim CD, Scott AF, Canadeo LA and Huibregtse JM: Extracellular ISG15 signals cytokine secretion through the LFA-1 integrin receptor. Mol Cell 68: 581-590.e5, 2017.
24. D'Cunha J, Knight E Jr, Haas AL, Truitt RL and Borden EC: Immunoregulatory properties of ISG15, an interferon-induced cytokine. Proc Natl Acad Sci USA 93: 211-215, 1996.
25. Forys JT, Kuzmicki CE, Saporita AJ, Winkeler CL, Maggi LB Jr and Weber JD: ARF and p53 coordinate tumor suppression of an oncogenic IFN-β-STAT1-ISG15 signaling axis. Cell Rep 7: 514-526, 2014.
26. Hadjivasiliou A: ISG15 implicated in cytoskeleton disruption and promotion of breast cancer. Expert Rev Proteomics 9: 7, 2012.
27. Cerikan B and Schiebel E: DOCK6 inactivation highlights ISGylation as RHO-GTPase balancer. Cell Cycle 16: 304-305, 2017.
28. Burks J, Reed RE and Desai SD: ISGylation governs the oncogenic function of Ki-Ras in breast cancer. Oncogene 33: 794-803, 2014.
29. Qiu X, Hong Y, Yang D, Xia M, Zhu H, Li Q, Xie H, Wu Q, Liu C and Zuo C: ISG15 as a novel prognostic biomarker for hepatitis B virus-related hepatocellular carcinoma. Int J Clin Exp Med 8: 17140-17150, 2015.
30. Yan W, Shih JH, Rodriguez-Canales J, Tangrea MA, Ylaya K, Hipp J, Player A, Hu N, Goldstein AM, Taylor PR, et al: Identification of unique expression signatures and therapeutic targets in esophageal squamous cell carcinoma. BMC Res Notes 5: 73, 2012.